ELSEVIER

Biophysical Chemistry 127 (2007) 51 – 63

Biophysical Chemistry

http://www.elsevier.com/locate/biophyschem

Stability of proteins in the presence of carbohydrates; experiments and modeling using scaled particle theory

Thomas F. O'Connor *, Pablo G. Debenedetti, Jeffrey D. Carbeck

Department of Chemical Engineering, Princeton University, Princeton, NJ 08544, United States

Received 21 August 2006; received in revised form 10 December 2006; accepted 10 December 2006
Available online 14 December 2006

Abstract

The effects of sucrose and fructose on the free energy of unfolding, $\Delta G_{N\rightarrow D}$, and on the change in hydrodynamic radius, R_H, upon unfolding were measured for RNase A and α-lactalbumin. Recently we analyzed the results for RNase A and showed that the effects of the carbohydrates on the protein's thermal stability can be accurately accounted for by scaled particle theory (SPT), and are thus largely entropic in nature. In this paper we extend this analysis to α-lactalbumin and demonstrate the generality of this finding. We also investigate the relationship between SPT and the thermodynamic formalism of preferential interactions. The preferential binding parameters calculated using SPT are in excellent agreement with experimentally measured values available in the literature. This agreement is expected to hold as long as enthalpic interactions between the cosolute and the protein are not important, as appears to be the case here. Finally we use the experimental data and SPT to calculate the change in the number of sugar molecules excluded from the protein surface during unfolding from knowledge of the preferential binding parameter for the native and denatured state of the protein.

Keywords: Protein stability; Carbohydrate; Scaled particle theory; Preferential interactions; Capillary electrophoresis

1. Introduction

Understanding how a protein's environment in solution affects its stability and thus its activity is important because the production, processing, and utilization of proteins in nature and biotechnology occur under solution conditions far removed from dilute aqueous buffers. Nature uses high concentrations of organic molecules, including carbohydrates, to protect organisms from environmental stresses [1]. Biomolecular interactions *in vivo* occur in crowded intracellular environments [2,3].

Carbohydrates are a class of organic molecules that have been shown to preferentially increase the stability of the native state of proteins over that of their denatured states [4]. This enhancement of stability typically increases with concentration of the sugar. The mechanisms by which these molecules increase protein stability are not fully understood.

Timasheff has described the effects of cosolutes, including carbohydrates, on protein stability in terms of preferential interactions between the protein, water, and the cosolute [5,6]. When a cosolute is added to a protein solution there is a perturbation in the chemical potentials of the protein and cosolute, which Timasheff has labeled the preferential interaction parameter. The observable manifestation of the change in chemical potential is the preferential binding parameter, $(\partial m_3/\partial m_2)_{T,P,\mu_3}$ where m is the molality of species i. Subscript 2 refers to the protein; water and the cosolute are represented as components 1 and 3, respectively, in accordance with the Scatchard notation [7]. The binding parameter is a measure of the difference in the cosolute concentration in the vicinity of the protein compared to the bulk solution [5]. It has been shown that molecules that are classified as protein stabilizers (including carbohydrates) are generally excluded from the protein surface: i.e. the concentration of the stabilizer is higher in the bulk solution then near the protein [8–10]. Preferential interaction is a thermodynamic formalism and does not by itself provide a molecular understanding of why some molecules are preferentially excluded from a protein's surface.

One potential explanation is molecular crowding. Minton has shown that high fractional volume occupancy has a

* Corresponding author. Tel.: +1 703 846 3769; fax: +1 703 846 1086.
E-mail address: thomas.f.oconnor@exxonmobil.com (T.F. O'Connor).

0301-4622/$ - see front matter © 2007 Elsevier B.V. All rights reserved.
doi:10.1016/j.bpc.2006.12.004

significant effect on the rates and equilibria of macromolecular reactions including protein folding [11,12]. These effects arise from nonspecific excluded volume interactions. These interactions progressively inhibit, with increasing extent of crowding, any conformational change of a protein that increases its effective volume, such as protein unfolding [12]. Molecular crowding theories are entropic in nature and do not consider enthalpic interactions between the crowding species and the protein.

Recently researchers have attempted to dissect the experimentally measured increase in stability into entropic and enthalpic components [4,13,14]. Schellman has described the impact of cosolutes on protein stability as a balance between contact interaction and excluded volume. In this approach, the entropic contribution to the incremental change in the free energy of denaturation upon the addition of sugar is viewed as being solely due to the excluded volume interactions, while the enthalpic contribution is due to a solvent exchange mechanism. To quantify these effects Schellman demonstrated that both the excluded volume and direct interaction could be extracted in a unified manner from the McMillan–Mayer formula for the second virial coefficient [14]. In this work the change in excluded volume upon unfolding was estimated from changes in solvent-accessible surface area (SASA). The SASA for the native states was calculated from the protein crystal structure, while the SASA for the denatured states was taken from the estimates developed by Creamer et al. [15].

Davis-Searles et al. and Saunders et al. used scaled particle theory (SPT) to calculate the entropic component of the effect of carbohydrates on protein stability [4,13]. SPT predicts the free energy of solvation of the protein in terms of the work of forming a cavity in the solution large enough to accommodate the protein, where the solution is modeled as mixture of hard spheres of different sizes [16]. The enthalpic contribution was then calculated by subtracting the entropic contribution from the measured change in stability [4,13]. SPT requires the hard sphere radii for the protein in both the native and denatured states. In the aforementioned studies, protein radii were estimated from SASA [4,13]. Radii of the native proteins were calculated from SASA estimated from crystal structures, while those of denatured proteins were calculated assuming SASA twice as large as those of the native protein. Both of these studies found that excluded volume interactions contribute to the stabilization of the native state and direct interactions between the protein and cosolute contribute to destabilization [4,13,14].

Other studies have shown that in the case of carbohydrates the major contribution to the cosolute's impact on protein stability is entropic in nature, while enthalpic interactions play only a minor role. Winzor and coworkers have had some success predicting the impact of carbohydrates on the stability and binding of proteins by including only the excluded volume interaction term of the second virial coefficient [17]. In a previous study we demonstrated that the effects of sucrose and fructose on the thermal stability of RNase A can be accurately accounted for by SPT, and are thus entropic in nature [18]. We used experimentally determined values of the effective hydrodynamic radius, R_H, as estimates of the hard sphere radii of native and denatured proteins [18]. The use of measured radii is important because the conformation of the denatured state can change significantly with solution conditions (pH, ionic strength, temperature, and concentration of chemical denaturants). This analysis was performed using a combination of capillary electrophoresis (CE) and protein charge ladders [19], collections of protein derivatives that differ incrementally in the number of chemically modified charge groups [18]. This approach provides information on both the thermodynamics (i.e., $\Delta G_{N\rightarrow D}$) and structural changes (i.e., R_H of proteins in both the native and denatured states) associated with stability, in a single set of experiments [18,20].

In this paper we have extended these experiments to another protein, α-lactalbumin, to demonstrate the generality of our previous finding. Secondly, we demonstrate the relationship between SPT and the thermodynamic formalism of preferential interactions. The preferential binding parameters calculated using SPT are in excellent agreement with experimentally measured values available in the literature. Thus we show that SPT provides a useful microscopic model of experimental preferential interaction parameters for carbohydrates. This model will be valid only when enthalpic interactions between the cosolute and the protein are not important, as appears to be the case with carbohydrates. Finally we calculate the change in the number of sugar molecules excluded from the protein surface during unfolding from the preferential binding parameter for the native and denatured state of the protein.

The paper is structured as follows. In the section titled Experimental methods we summarize the techniques used to measure $\Delta G_{N\rightarrow D}$, and the change in R_H of the protein upon unfolding. In Results we compare data for these quantities measured in the presence of sucrose and fructose for both RNase A and α-lactalbumin. In the Discussion section these results are analyzed using SPT and the robustness of this analysis is examined, the importance of the denatured conformation and the formation of a protein-solvent interface in determining a sugar's impact on protein stability are shown, and preferential binding parameters are calculated using SPT. The main findings are summarized in the Conclusions section.

2. Experimental

2.1. Materials

Fused silica capillaries (i.d. = 50 μm) were obtained from Polymicro Technologies (Phoenix, AZ). α-lactalbumin (α-LA) (type I, from bovine milk, calcium saturated), Ribonuclease A (RNase A), Trizma base, and glycine were purchased from Sigma (St. Louis, MO). Poly-diallyldimethylammonium chloride (PDADMAC) (high molecular weight, 20 wt.% solution), acetic anhydride, 1,4-dioxane, and *p*-methoxybenzyl alcohol (PMBA) were purchased from Aldrich (Milwaukee, WI). Sodium chloride and 1 N NaOH were obtained from Fisher Scientific (Fair Lawn, NJ). All chemicals were used as received and all solutions were made using 18 MΩ deionized water.

2.2. Synthesis of charge ladders

Protein charge ladders of α-LA and RNase A were made by the selective acetylation of Lys ε-amino groups at pH 12 [19]. Proteins were dissolved in water at a concentration of ~0.1 mM, and 10 vol.% of 0.1 N NaOH was added to bring the pH to ~12. 5 μL of a 1 vol.% acetic anhydride solution (in 1,4 dioxane) were added to 100 μL of the protein solution. The reaction products were analyzed by capillary electrophoresis without further purification. The change in charge due to acetylation, ΔZ, of Lys ε-NH_3^+ groups ($pK_a \approx 10.4$) is ~1 at the pH of our experiments (pH 8.4). We characterized the charge ladders of α-LA using the first six (out of 13) rungs of the ladder. Later rungs were excluded due to lower concentrations and a greater degree of peak broadening, relative to the earlier rungs of the ladder. The charge ladders of RNase A were characterized using the first three rungs of the ladder because subsequent rungs were oppositely charged and were not detected.

2.3. Capillary electrophoresis

Capillary electrophoresis (CE) experiments were run on a Beckman P/ACE 5000. The intrinsic capillary cooling system was redirected through an external bath that was operated between 20 and 90 °C. The coolant used was Flourinert-77, purchased from 3M (St. Paul, MN). Capillaries ranging in total length from 27 to 47 cm were used. Proteins were denatured by increasing the temperature of the capillary.

The electrophoresis buffer for experiments conducted with α-LA was 25 mM Tris, 192 mM Gly (pH 8.4), 25 mM NaCl, 35 μM $CaCl_2$, and varying concentrations of carbohydrates (ranging from 0 to 30 wt.%) while the run buffer for RNase A experiments was 25 mM Tris, 192 mM Gly (pH 8.4), 30 mM NaCl, and varying concentrations of carbohydrates (ranging from 0 to 25 wt. %). The interactions between RNase A and the negatively charged silica had to be minimized because the protein is positively charged at the pH at which the experiments were conducted. To reduce these interactions, PDADMAC was physically absorbed on to the walls of the capillary. The coating procedure has been detailed elsewhere [21]. Capillaries coated in this manner underwent separations in the "reverse polarity" mode with the cathode at the inlet.

An injection sample, with a total volume of 100 μL, was prepared by diluting the charge ladder 10-fold in electrophoresis buffer. PMBA was added to the injection sample at a concentration of 0.0025 vol.% as a neutral marker of electroosmotic flow. Injection time was varied from 4 to 6 s to account for the increase in viscosity due to the addition of carbohydrates. Separations were performed at an applied potential of 15 kV. Values of electrophoretic mobility were determined from $v_{elec} = (l_t l_O / V)(1/t_{nm} - 1/t_p)$, where t_p is the migration time of the protein, t_{nm} is the time of emergence of the neutral marker, l_t is the total length of the capillary, l_o is the length to the detector, and V is the applied voltage. Values of mobility were corrected for changes in viscosity due to changes in temperature by multiplying the measured mobility by $\eta(T)/\eta_o$ where η is the viscosity of the electrophoretic run buffer at the given temperature and η_o is the viscosity of the run buffer at 25 °C. Viscosity values were measured with a capillary viscometer.

2.4. Analysis of protein charge ladders

The effective hydrodynamic radius of a protein, R_H, is defined as the radius of a sphere that has the same translational coefficient of friction as the protein. Plots of v_{elec} of the rungs of the charge ladder *vs* $n\Delta Z$ at a given temperature were fit using a combination of Debye–Hückel theory and Henry's model of electrophoresis [22]

$$v_{elec}^{n} = \frac{e(Z_{CE} + n\Delta Z)}{6\pi\eta R_H} \frac{f_1(\kappa R_H)}{1 + \kappa R_H} \tag{1}$$

In the above equation, v_{elec}^{n} is the electrophoretic mobility of the nth rung of the charge ladder, Z_{CE} is the net effective charge that gives rise to the electrophoretic motion of the protein, $n\Delta Z$ is the total change in charge due to acetylation for nth rung of the charge ladder, R_H is the effective hydrodynamic radius of the protein, κ the inverse Debye length, η the viscosity of the buffer, e is the fundamental unit of charge, and f_1 is a function of κR_H that describes the effects of the protein on the local electric field. $f_1 = 1$ when $\kappa R_H < 1$ (the Hückel limit) and $f_1 = 3/2$ when $\kappa R_H > 10$ (the Hückel–Smoluchowski limit). Between the two limiting cases, f_1 is calculated using Eq. (2) [22].

$$f_1(\kappa R_H) = \left(1 + \frac{(\kappa R_H)^2}{16} - \frac{5(\kappa R_H)^3}{48} - \frac{(\kappa R_H)^4}{96} + \frac{(\kappa R_H)^5}{95} - \frac{11}{16} e^{\kappa R_H} \int_{\infty}^{\kappa R_H} \frac{e^{-r}}{r} dr\right) \tag{2}$$

The slope of the best-fit v_{elec}^{n} *vs.* $n\Delta Z$ line provides R_H for the unmodified protein. Eqs. (1) and (2) were solved together using a trial and error approach.

An assumption inherent in this analysis is that this size and shape of the protein does not change upon the acetylation of the amino groups on the protein's surface. This assumption has been called into question [23] in view of the fact that different mutants with the same net charge exhibit different electrophoretic mobilities [24]. However it has been shown that increasing the molecular weight and thus the size of the acetylating agent has no effect on the electrophoretic mobility of the different rungs of the charge ladder [25]. This finding indicates that the chemical modification of the protein's surface has little to no effect on the protein's size and shape.

2.5. Taylor's analysis of dispersion

Sharma et al. have described a method for measuring the diffusivity of solutes using Taylor's analysis of dispersion in a commercial CE instrument [26]. All experiments were conducted on a Beckman P/ACE 5510 CE instrument. Capillaries ranging in length from 27 to 37 cm with an inner diameter of 50 μm were used. For analysis of solution fronts the inlet end of the capillary was transferred to the vial containing the solute in

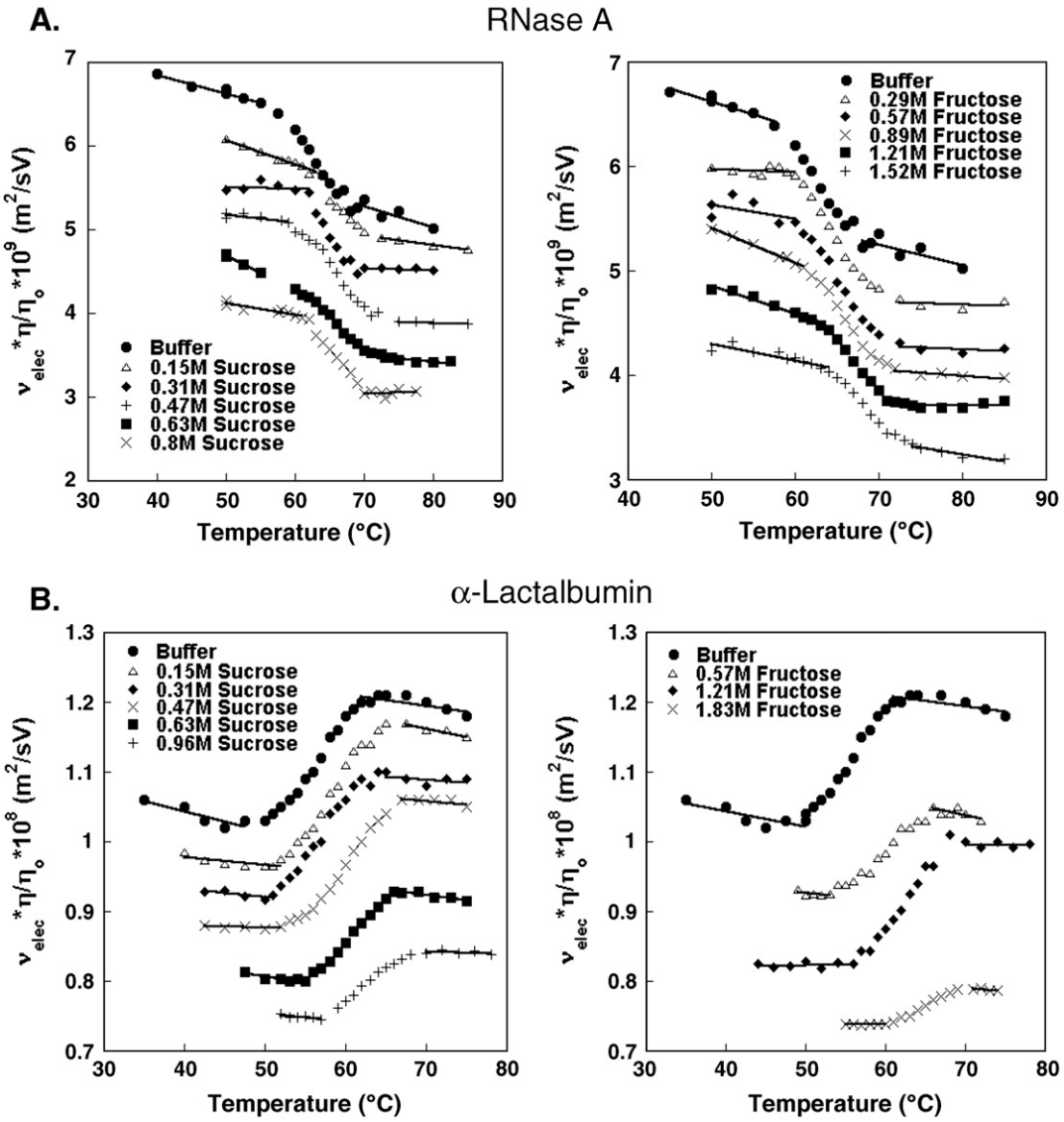

Fig. 1. Temperature dependence of the electrophoretic mobility of A) RNase A and B) α-lactalbumin in buffer solution and in the presence of sucrose and fructose. The measured electrophoretic mobility has been corrected for changes in viscosity with temperature by multiplying the mobility by $\eta(T)/\eta_o$ where η is the viscosity of the electrophoretic run buffer at the given temperature and η_o is the viscosity of the run buffer at 25 °C.

solution and a pressure drop of 0.5 psi was applied across the capillary. The mean residence time, t_R, and σ, a measure of the sharpness of the front, are determined by fitting the normalized concentration profile to the following equation [27].

$$\frac{C}{C_o} = \frac{1}{2} \pm \frac{1}{2}\mathrm{erf}\left(\frac{(t-t_R)}{\sigma\sqrt{2}}\right) \tag{3}$$

The diffusivity of the solute, D, can then be determined from Eq. (4) if two conditions are met [28]: (i) the dimensionless residence time, $\tau = Dt_R/R_C^2 > 1.4$ and (ii) the Péclet number, $Pe = u_o R_c/D > 70$ where R_c is the radius of the capillary and u_o the mean fluid velocity,

$$D = \frac{R_c^2 t_R}{24\sigma^2} \tag{4}$$

The diffusivity is related to R_H through the Stokes–Einstein equation:

$$R_H = \frac{kT}{6\pi\eta D} \tag{5}$$

In the above equation k is Boltzmann's constant and T is the absolute temperature.

Values of R_c were determined using a volumetric technique. Water was pressurized through a capillary of total length L_T for a period of at least 20 min to minimize effects of the initial ramp in fluid velocity. The volumetric flow rate, Q, was obtained by measuring the mass of water that passed through the capillary in the allotted time for a given pressure drop, Δp, and then using the density of water to convert to

volume. The radius of the capillary was then determined using the Hagen–Poiseuille law.

$$R_c = \left(\frac{8L_T\eta Q}{\pi\Delta p}\right)^{\frac{1}{4}} \quad (6)$$

3. Results

3.1. Thermodynamic results

Recently a growing number of studies have utilized CE to monitor the folding/unfolding transitions of proteins [20,29–36]. CE offers the advantages of high sensitivity, minute sample size, quick analysis time, and high resolution [37]. Thermodynamic parameters determined from CE have been shown to be in good quantitative agreement with those determined from CD and calorimetry [30,31]. In this study the effects of sucrose and fructose on the thermodynamics of unfolding of RNase A and α-LA were measured by monitoring the electrophoretic mobility (v_{elec}) of the two proteins as a function of temperature. Fig. 1 shows shifts in the thermal transition curves of the two proteins upon the addition of sugar. The values of v_{elec} plotted in Fig. 1 have been corrected for changes in viscosity with temperature by multiplying the measured mobility by the ratio of $\eta(T)/\eta_o$ where η is the viscosity of the electrophoretic run buffer at the given temperature and η_o is the viscosity of the run buffer at 25 °C. Upon the addition of sugar, the mobility curves are shifted to lower values because the viscosity of the run buffer increases.

We assumed that the thermal unfolding of both proteins could be approximated as a two-state transition. It has been shown that α-LA forms a molten globule under acidic conditions [38,39]. The conditions used in the present experiments, higher values of pH and an excess concentration of $CaCl_2$, suppress the formation of the molten globule and shift α-LA to a two-state folding pathway [40]. The temperature dependence of v_{elec} for the pre-transition and post-transition regions was estimated by fitting the data to a line [41]. The pre-transition and post-transition baselines are shown in Fig. 1. The pre- and post-baselines are different for each sugar concentration. Even if the mobility is adjusted for changes in viscosity upon the addition of sugar, the baselines are still different because the addition of sugar changes other solution properties such as the dielectric constant that affects v_{elec} of the protein.

The equilibrium constant (K) for the unfolding reaction at a given temperature is then described by the following equation,

Table 1
Comparison of thermodynamic data obtained from DSC and CE

	RNase A		α-Lactalbumin	
	DSC [a]	CE [b]	DSC [c]	CE [b]
ΔH_m (kcal/mol)	102.3 (5.1)	98 (4.9)	70 (3.5)	69 (1.0)
T_m (K)	334.8 (0.2)	335.6 (0.2)	337.3 (0.2)	329.1 (0.2)
ΔC_p (kcal/mol K)	1.15 (0.06)	1.3 (0.7)	1.7 (0.2)	2.1 (0.45)

[a] pH 7. Ref. [42].
[b] pH 8.4. This work.
[c] pH 8 Ref. [43].

Table 2
Effects of carbohydrates on the stability and hydrodynamic radius of RNase A and α-lactalbumin[a]

	T_m (°C)	$\Delta G_{N\rightarrow D}$ (kcal/mol)	$R_{H,N}$ (Å)	$R_{H,D}$ (Å)
RNase A				
Buffer	62.6 (0.1)	8.2 (0.2)	21.2 (0.3)	27.5 (0.3)
0.15 M sucrose	63.6 (0.1)	9.1 (0.2)		
0.31 M sucrose	64.7 (0.2)	9.5 (0.2)	21.9 (0.3)	28.2 (0.3)
0.47 M sucrose	65.9 (0.1)	10.2 (0.2)		
0.63 M sucrose	66.5 (0.2)	10.6 (0.2)	22.2 (0.3)	28.0 (0.3)
0.80 M sucrose	67.1 (0.2)	11.1 (0.2)		
0.29 M fructose	63.9 (0.1)	9.1 (0.2)		
0.57 M fructose	64.5 (0.2)	9.5 (0.2)	21.7 (0.3)	28.0 (0.3)
0.89 M fructose	66.0 (0.2)	10.1 (0.2)		
1.21 M fructose	66.5 (0.1)	10.5 (0.2)	22.0 (0.3)	28.0 (0.3)
1.52 M fructose	68.0 (0.2)	11.2 (0.2)		
Δ-Lactalbumin				
Buffer	56.1 (0.1)	3.3 (0.2)	21.4 (0.5)	27.5 (0.5)
0.15 M sucrose	56.3 (0.1)	3.8 (0.2)		
0.31 M sucrose	57.5 (0.1)	4.6 (0.2)	21.0 (0.5)	27.7 (0.5)
0.47 M sucrose	59.0 (0.2)	5.3 (0.2)		
0.63 M sucrose	60.5 (0.2)	5.7 (0.2)	21.5 (0.5)	28.4 (0.5)
0.96 M sucrose	62.4 (0.2)	7.0 (0.2)		
0.57 M fructose	60.0 (0.1)	4.5 (0.2)	21.4 (0.5)	27.7 (0.5)
1.21 M fructose	61.6 (0.2)	5.6 (0.2)	21.2 (0.5)	28.2 (0.5)
1.83 M fructose	63.2 (0.2)	6.9 (0.2)		

[a] T_m is the melting temperature, $\Delta G_{N\rightarrow D}$ is the free energy of unfolding at 25 °C, $R_{H,N}$ is the hydrodynamic radius of the protein in the native state and $R_{H,D}$ in the denatured state. Values in parentheses are estimates of standard error of the data. Hydrodynamic radius measurements of RNase A were made using charge ladders while hydrodynamic radius values for α-lactalbumin were determined using dispersion analysis.

where $v^N_{elec}(T)$ and $v^D_{elec}(T)$ are the mobilities of the native and denatured protein, respectively, at that temperature.

$$K(T) = \frac{v^N_{elec}(T) - v_{elec}(T)}{v_{elec}(T) - v^D_{elec}(T)} \quad (7)$$

The values of $\Delta G_{N\rightarrow D}$ can be easily calculated from values of K and are assumed to follow the Gibbs–Helmholtz equation, Eq. (8), the underlying assumptions for which are that the unfolding reaction is a two-state process, and the change in heat capacity upon unfolding, Δc_p, is independent of temperature. Three thermodynamic parameters were used to fit each data set: the enthalpy of melting, ΔH_m, the melting temperature, T_m, and Δc_p.

$$\Delta G_{N\rightarrow D}(T) = -RT\ln K = \Delta H_m(1 - T/T_m) + \Delta c_p[(T - T_m) - T\ln(T/T_m)] \quad (8)$$

Table 1 compares the thermodynamic parameters for the unfolding of RNase A and α-LA at pH 8.4 obtained from CE to literature values at pH 7 for RNase A and pH 8 for α-LA obtained using differential scanning calorimetry (DSC) [42,43]. For RNase A there is excellent agreement between the values of ΔH_m and T_m measured using the two techniques. In the case of α-LA, there is excellent agreement between the values of ΔH_m but the T_m values differ by ~8 K. This is due to the difference in the concentration of calcium ions used in Ref. [43] and in our experiments. As explained in Ref. [43],

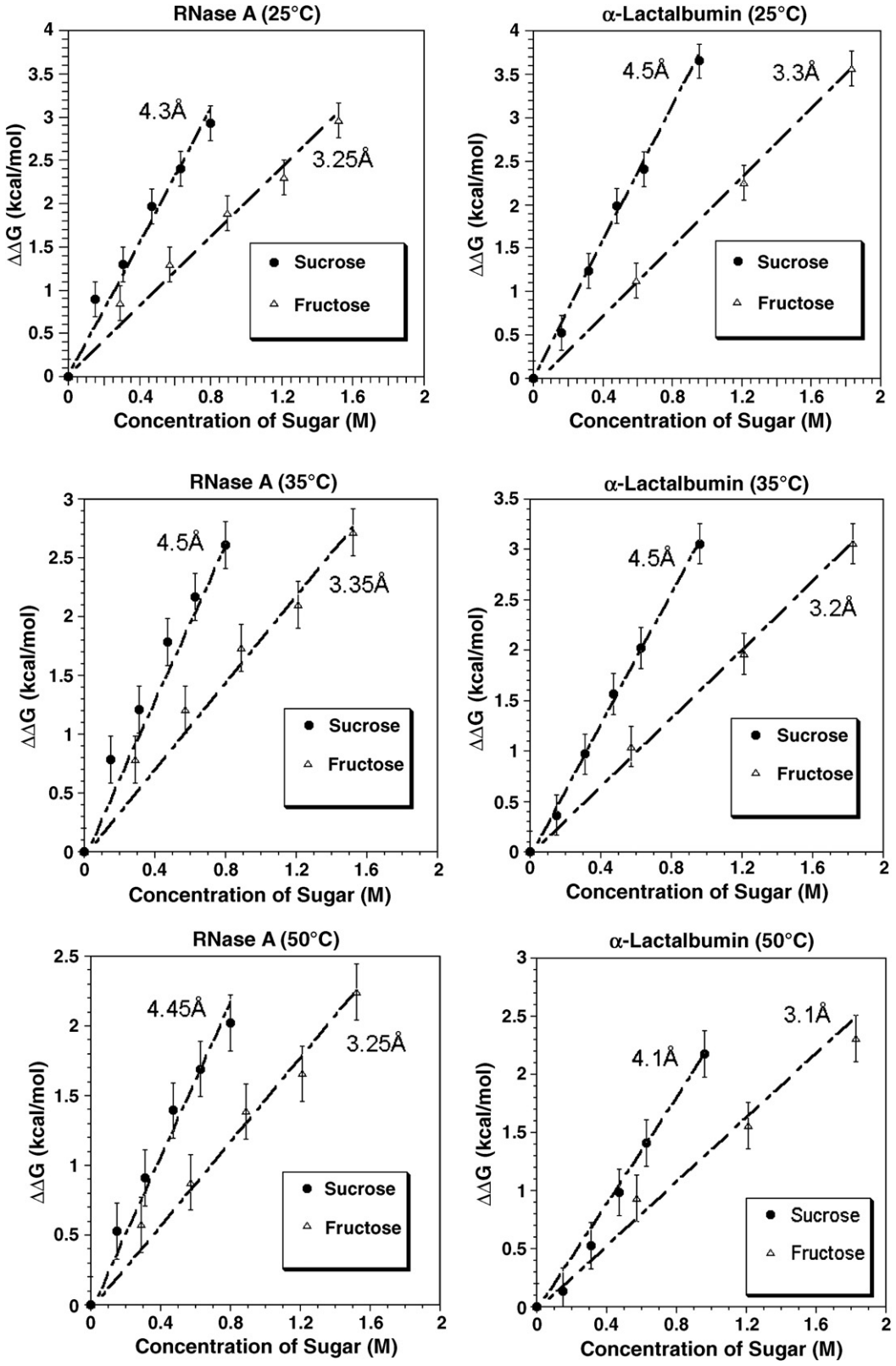

Fig. 2. Values of $\Delta\Delta G$, the difference in $\Delta G_{N\rightarrow D}$ measured in the presence of sugars and in buffer, for RNase A and α-lactalbumin as a function of molar concentration of sugar at three different temperatures: 25 °C, 35 °C, and 50 °C. Lines are predictions using scaled particle theory with fitted values of effective sugar radii shown in each case.

the T_m of α-LA is a sensitive function of calcium ion concentration. There is also very good agreement between the two values of Δc_p. We note, however, that the appreciable uncertainty in the value of Δc_p determined using CE is indicative of the difficultly of obtaining reliable heat capacity values from a two-state fit. As previously noted [44], methods that fit experimental data to a two-state model provide accurate values of T_m and ΔH_m, given that the assumption of two-state folding is realistic, but less accurate values of Δc_p. Values of ΔH_m are determined from the slope of the experimental data while values of Δc_p are related to the second derivative of the curve fit to the experimental data.

Values of T_m and $\Delta G_{N\rightarrow D}$ for both proteins in the presence of different concentrations of sucrose and fructose are listed in Table 2. The addition of both carbohydrates results in a shift in the T_m of RNase A and α-LA to higher values, and an increase in the free energy barrier to unfolding at 25 °C. Sucrose and fructose increased the T_m of RNase A by 5.6 °C and 3.6 °C per mole of sugar added, respectively, and that of α-LA by 6.6 °C and 3.9 °C per mole of sugar added, respectively. $\Delta G_{N\rightarrow D}$ increases approximately linearly with concentration of sugar; thus, the degree to which a cosolute impacts the change in free energy can be quantified by the slope of $\Delta G_{N\rightarrow D}$ with respect to sugar concentration. Doing so yields values for RNase A of 3.6 kcal/mol per mole of sucrose and 2.0 kcal/mol per mole of fructose, and, for α-LA, 3.8 kcal/mol per mol of sucrose and 1.9 kcal/mol per mole of fructose. Both measures of stability (T_m and $\Delta G_{N\rightarrow D}$) show that, on a per mole basis, the disaccharide sucrose stabilizes both proteins to a greater extent than the monosaccharide fructose. To further quantify the effects of sugars on stability, $\Delta\Delta G$ was calculated by subtracting values of $\Delta G_{N\rightarrow D}$ for the protein in buffer without carbohydrates from the corresponding quantity obtained in the presence of sugar. In Fig. 2A and B values of $\Delta\Delta G$ are plotted as a function of molar concentration of sugar for RNase A and α-LA, respectively.

3.2. Structural results

We measured values of R_H for the native and denatured states of both proteins, using a combination of CE and charge ladders or dispersion analysis as described in the experimental methods section. The results are presented in Table 2. Fig. 3 shows a comparison of R_H values measured using charge ladders to those determined through dispersion analysis for α-LA in buffer. The two methods are in excellent agreement for the native state and within 5% of each other for the denatured state of the protein. It is not surprising that there is a greater discrepancy for the denatured state, which probably deviates to a greater extent from the spherical geometry assumed in the models.

There are small increases in the R_H of the native state of both proteins upon the addition of sugar, as measured by the combination of CE and charge ladders. This trend is not reproduced by dispersion analysis, which showed no change in R_H of the native state of α-LA upon the addition of sugar. It is our contention that there is no actual change in the hydrodynamic size of the two proteins studied upon addition of sugar. The differences between the two measurements can be rationalized by considering the assumption that the change in charge upon acetylation, ΔZ, is −1. Inherent in this statement is the assumption that changing the charge of one residue on the surface of a protein has no effect on the pK_a of the surrounding ionizable residues. There have been several studies that demonstrate that, due to charge regulation [21,45], this is not always the case. Upon addition of 20 wt.% sugar the dielectric constant of the solution, as calculated by a simple mixing rule, decreases by approximately 20%. Thus the strength of electrostatic interactions should increase by a corresponding amount. This could cause ΔZ to deviate further from −1, which would result in an increase in the value of R_H.

To test this hypothesis, charge ladder experiments were conducted at several higher concentrations of salt at a given sugar concentration. Increasing the salt concentration increases the inverse Debye length, and thus the length over which electrostatic interactions are important is decreased. This will reduce deviations of ΔZ from −1 due to charge regulation. Values of R_H so obtained decreased as the concentration of salt

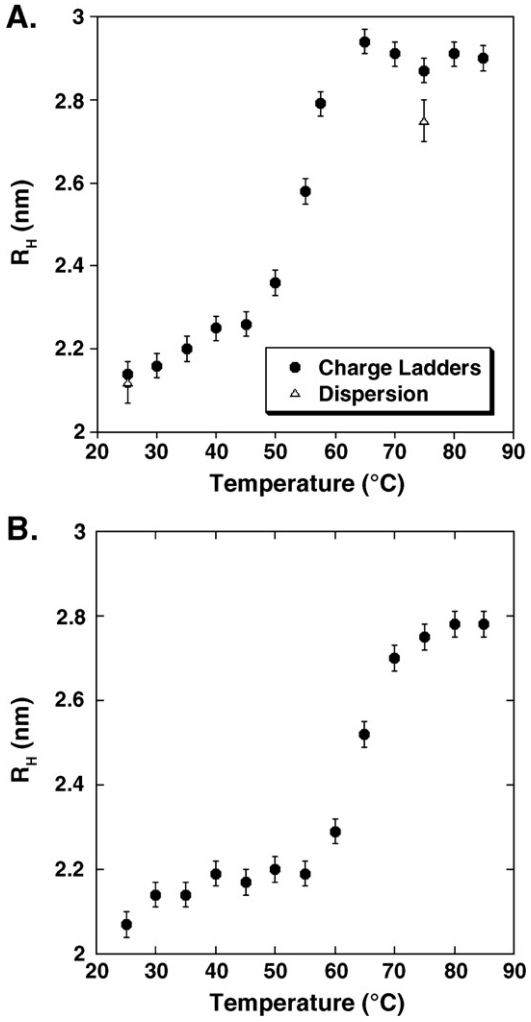

Fig. 3. A) The hydrodynamic radius of α-lactalbumin in pH 8.4 buffer as a function of temperature, measured using charge ladders and dispersion analysis. B) The hydrodynamic radius of RNase A in pH 8.4 buffer as a function of temperature, measured using charge ladders.

increased until they leveled off at a value in good agreement with the value of R_H obtained in buffer using both charge ladders and dispersion analysis (data not shown). The advantage of using charge ladders compared to dispersion analysis is that it yields information about R_H and the net charge of the protein in a single set of electrophoresis experiments. This information has made charge ladders extremely useful in determining the role of electrostatics in protein folding [20], and protein-ligand binding [46,47]. From the results presented here it appears that ΔZ is close −1 for both proteins in their respective buffers, but begins to deviate from this value upon addition of sugar.

The results from both charge ladders and dispersion show no change in the values of R_H for the denatured states of both proteins upon the addition of carbohydrates. Bolen has shown that the denatured state of reduced and carboxamidated RNase A contracts in the presence of protecting cosolutes [48]. We see no evidence of this effect over the range of sugar concentrations used in this study. We note, however, that the two proteins investigated have four disulfide bonds each and these remain intact in the denatured state under the conditions explored here. These disulfide bonds do not prevent the proteins from expanding upon denaturation, as we indeed measure an increase in RNase A's and α-LA's R_H upon unfolding. We do observe, however, more compact denatured states than are commonly measured in the absence of disulfide bonds [48]. It appears that this more compact denatured state is resistant to further compression due to the presence of increasing concentrations of these sugars.

In general there is less concern about ΔZ deviating from −1 in the denatured state because charged residues are further apart than in the native state. In support of this line of reasoning, the R_H values for the denatured state of RNase A are unchanged when the concentration of salt is increased at a given sugar concentration. Also, the measurements made using charge ladders report the same trend as those made using dispersion analysis, which is free from any assumption about values of ΔZ.

4. Discussion

4.1. Analysis of results using Scaled Particle Theory (SPT)

To rationalize the effects of carbohydrates on the thermal stability of the two proteins studied we used a simple physical picture of the free energy of solvation of proteins: contributions of sugars to the enthalpy of solvation are ignored and only entropic effects are considered. SPT, which models the solution as a mixture of hard spheres, was used to calculate these entropic effects [16]. SPT predicts the free energy of solvation of the protein in terms of the work of forming a cavity in the solution large enough to accommodate the protein. The reversible work of cavity formation, w, is expressed as a third-order polynomial in the radius of the cavity, R and is given by

$$\frac{w}{kT} = -\ln(1-S_3) + \frac{6S_2}{(1-S_3)}R + \left[\frac{12S_1}{(1-S_3)} + \frac{18S_2^2}{(1-S_3)^2}\right]R^2 + \frac{4}{3}\pi\frac{PR^3}{kT} \quad (9)$$

where P is the pressure and S_j is given by

$$S_j = \frac{\pi}{6}\sum_{i=1}^{m} \rho_i(2R_i)^j; j = 1,2,3 \quad (10)$$

In Eq. (10), ρ_i and R_i are the number density and the hard sphere radius of species i. The number density of water was adjusted as a function of cosolute concentration as prescribed by Berg [49].

We used Eq (9) to calculate the difference in w for the protein in water and in the sugar solution. In the application of Eq. (9) the true pressure of the solution (1 atm) is used instead of the hard sphere pressure. P is then the same for water and the sugar solution and thus the term proportional to R^3 cancels. We calculated $\Delta\Delta G$ as the difference in values of $(w_D - w_N)$ in the presence of sugar and in water. SPT thus predicts the change in stability of the protein due to the contributions that the sugars make to the entropy of solvation of the native and denatured states of the protein.

In the version of SPT used in this study water is treated explicitly [49]. This approach requires values of the hard sphere radii for water, sugars, and for the protein in both the native and denatured states. We used experimentally determined values of R_H for both proteins in their native and denatured states as estimates of their hard sphere radii. We used 1.38 Å for water's hard sphere radius [13]. Sugar radii were fitted to the experimental data for the two proteins independently. The fits of the model to the experimental data are shown in Fig. 2. This analysis yielded values of 4.3 Å for sucrose and 3.25 Å for fructose for the stabilization of RNase A, and 4.5 Å for sucrose and 3.3 Å for fructose for the stabilization of α-LA. These results are in good agreement with values reported previously [50] of 3.9–4.5 Å for sucrose and 3.2–3.9 Å for glucose, a monosaccharide similar in size to fructose. SPT analysis of the impact of sucrose and fructose on the stability of the two proteins was also conducted at 35 °C and 50 °C. These results are also shown in Fig. 2. The values of sugar radii obtained at the higher temperatures from the SPT fit to the thermodynamic data differ only slightly from those obtained at 25 °C. The average values of the sugar radii were determined to be 4.4 Å and 3.25 Å for sucrose and fructose, respectively.

Clearly, neither water nor the sugars are realistically spheres with no enthalpic interactions with the protein, which is also non-spherical, especially in the denatured state. In addition, the picture of proteins as impenetrable hard spheres is also an idealization. In spite of these simplifications, SPT is able to describe quantitatively the effects of these sugars on the stability of both RNase A and α-LA, as is shown in Fig. 2. These results suggest that geometric differences between carbohydrates play a predominant role in determining their relative ability to stabilize proteins against thermal denaturation.

4.2. Sensitivity of SPT to model parameters

Tang and Bloomfield have examined the uncertainty in predicted values of w due to the uncertainties in the model's parameters [50]. They have shown that calculated values of w

are very sensitive to the radii and densities of the solvent molecules. Here we examine how uncertainties in these parameters affect the results presented in this paper.

There is an appreciable range of experimental and theoretical values for the hard sphere radii of both fructose and sucrose: 3.2–3.9 Å for fructose and 3.9–4.5 Å for sucrose [50]. This range is probably due to the fact that the geometry of both sugars is non-spherical. Thus different methods for calculating the hard sphere radius yield different results. We examined the impact of this variation by using the lower and upper bounds of the sugars' radii to calculate values of $\partial\Delta G/\partial C_3$ for the unfolding of RNase A. The calculated effect of fructose on RNase's stability ranges from 1.9 to 2.9 kcal/mol per mole of sugar, while that of sucrose varies from 3.0 to 4.1 kcal/mol per mole of sugar, depending on the value of sugar radius used. Comparing these values to the experimental values of 2.0 and 3.6 for fructose and sucrose, respectively, we conclude that the analysis of the data using SPT yields results that do not vary by appreciable amounts when the radius of the carbohydrate is varied across its full range of reported values.

4.3. Comparison with published data

The experimental observations that the enhancement of stability increases with carbohydrate concentration and size are in agreement with published data [13,51]. The effects of sugars on protein stability have been previously explained in terms of excluded volume interactions. Shearwin and Winzor were able to predict the impact of sucrose on $\Delta G_{N\rightarrow D}$ for the acid unfolding of RNase A by considering only the excluded volume contribution to the second virial coefficient [17]. In the case of a dilute protein solution $\Delta\Delta G$ can be expressed in terms of the cross term second virial coefficient for the denatured and native protein, B_{23D} and B_{23N} respectively [52].

$$\Delta\Delta G = RT(B_{23,D}-B_{23,N})C_3 \tag{11}$$

where C_3 is the molar concentration of the cosolute. For an inert cosolute $B_{23,i}$ is the covolume of the cosolute and the protein in state i. For spherical cosolutes $B_{23,i}$ is given by

$$B_{23,i} = 4/3\pi N(R_{2,i}+R_3)^3 \tag{12}$$

where $R_{2,i}$ and R_3 are the radius of the protein in state i and the cosolute respectively and N is Avogadro's number.

Sasahara et al. were able to calculate the increase in stability of the molten globule state of cytochrome c compared to the completely unfolded protein in the presence of dextran, a carbohydrate polymer [44]. The approach used by Sasahara and coworkers was similar to the one used by Shearwin and Winzor except that dextran was treated as a cylinder instead of a spherical cosolute. The change in stability of 0.04 kJ/mol per g of dextran [44] is comparable to the values of 0.044 kJ/mol per g of sucrose and 0.046 kJ/mol per g of fructose measured in the present study. This suggests that the magnitude of the change in conformation upon unfolding is similar for the proteins in the two studies. This point will be discussed further in Section 4.4.

The good agreement between the predicted impact of dextran on the stability of cytochrome c and measured values might be due to the large size of the carbohydrate dextran. It was found that quantitative agreement between the covolume analysis and experimental data improved as the size of the sugar increased [53]. For the case of smaller cosolutes the covolume approach has been shown to significantly overestimate the impact of polyols on $\Delta G_{N\rightarrow D}$ including the impact of glycerol on the thermal unfolding of RNase A [17] and the effect of several sugars on the acid stability of ferricytochrome c [53]. This is in agreement with our calculations, which showed that the covolume analysis overpredicted values of $\partial\Delta\Delta G/\partial C_3$ by a factor of 50.

The explicit version of SPT has also been previously used to quantify the impact of sugars on protein stability due to excluded volume interactions. The predictions from this version of SPT have been in better quantitative agreement with experimental data [13,53]. Saunders et al. found there was still a discrepancy between calculated and measured values of $\partial\Delta\Delta G/\partial C_3$ for the thermal and acid unfolding of ferricytochrome c in the presence of various sugars [13]. The magnitude of this difference ranged between 1 and 4 kcal/mol for sucrose and was attributed to enthalpic interactions between the protein and carbohydrate molecules. Better quantitative agreement was achieved in the present study by using experimentally measured R_H values as estimates of the size of the denatured state. In previous studies the size of the denatured state was calculated from estimates of the solvent-accessible surface area (SASA) [13,53]. Even though better quantitative agreement was found using the current approach, the modeling of the denatured state in excluded volume calculations is still an open question [54].

Analyzing the changes in $\Delta G_{N\rightarrow D}$ using SPT along with the experimentally measured R_H values as estimates of the size of the native and denatured states of the protein has yielded values of sugar radii within the range of previously reported values for two different sugars with two different proteins at three different temperatures. However, the uncertainty in the SPT parameters, such as the value of the sugar radius, does not allow one to rule out the possibility that enthalpic interactions might play a role in the effect of sucrose and fructose on the thermal stability of RNase A and α-lactalbumin. It is interesting to note that in the case of sucrose these enthalpic interactions would be stabilizing and for the case of fructose, destabilizing.

4.4. Importance of the denatured state

Interactions between the denatured protein and the solvent are as important as those between the solvent and the native protein in determining stability. In order to predict the impact of changing solvent conditions on the stability of a protein, one needs information about its denatured state. The denatured state in general can′t be thought of as a random coil but instead consists of residual secondary structure and the structural properties of this state depend on the solvent conditions [55].

Both protein charge ladders and analysis of dispersion allow for the efficient determination of the hydrodynamic radius of a denatured protein under a wide variety of solution conditions.

These experiments provide low-resolution structural information that can be used to estimate the change in solvent accessible surface area (SASA) upon denaturation. This information is important because most models that aim to predict the impact of cosolutes on protein stability, including SPT, have the change in R_H or SASA upon denaturation as a key parameter. Thus the effect of a sugar on the stability of the protein is dependent upon the denatured configuration under a given set of conditions.

One example of the importance of the denatured configuration is the fact that the experimentally measured impact of the disaccharide sucrose on the stability of RNase A ($\Delta\Delta G$ of 3.6 kcal/mol per mole of sugar) is almost twice the previously reported value for sucrose ($\Delta\Delta G$ of 2.1 kcal/mol per mole of sugar) [8] and the disaccharide trehalose ($\Delta\Delta G$ of 1.9 kcal/mol per mole of sugar) [9]. Sucrose and trehalose are very similar in size, and thus, according to SPT, they should have the same impact on the stability of RNase A. The discrepancy between the values of $\Delta\Delta G$ measured by Timasheff and coworkers [8,9] and those reported in this study can be accounted for by the difference in the denatured state of RNase A under the solution conditions in which the different measurements were made. The sucrose and trehalose measurements reported in Refs. [8,9] were made under acidic conditions, where the radius of RNase A in the denatured state has been measured as 23.5 Å [56]. We measured the R_H of the thermally denatured state at pH 8.4 to be 27.5 Å. If we use values of 23.5 Å for the denatured state and 4.3 Å for the disaccharide, SPT predicts a $\Delta\Delta G$ value of 1.9 kcal/mol per mole of disaccharide, in agreement with the reported values [8,9]. As shown, varying solution conditions can alter the denatured state of the protein, and thus can have a significant effect on the impact a cosolute has on the protein's stability.

4.5. Importance of the protein-solvent interface

The SPT expression for work of cavity formation can be rewritten as shown in Eq. (13).

$$w = A + BR + CR^2 + \frac{4}{3}\pi R^3 p \tag{13}$$

In Eq. (13) the R^3 term represents the volume work required to create a cavity where p is the pressure of the fluid. The R^2 term is associated with surface free energy contribution. The R term represents the effect of the cavity's curvature on the surface free energy contribution and A is the work of inserting a point molecule into the solution [57]. Analyzing the relative contributions of the different terms in the SPT expression shows that the term associated with the surface work contributes 90–95% of the total value of w. The volume work doesn′t contribute to w because the p of the solution is the same in water and the water–sugar mixture. According to the model sucrose has a greater impact on $\Delta G_{N\rightarrow D}$ than fructose at the same molar concentration because the larger sugar, sucrose, makes a greater contribution to the unfavorable entropy of interface formation.

This result is consistent with previous observations that values of w are approximately proportional to the area of the protein-solvent interface [58,59]. Timasheff and coworkers have demonstrated that the denaturation of RNase A in the presence of carbohydrates occurs at a constant surface energy. They showed that the surface tension of the solution at the protein's T_m was constant [8,58]. In this work we have focused on another parameter of the protein's stability, $\Delta G_{N\rightarrow D}$ at 25 °C, and have used a microscopic model instead of a macroscopic solution property to describe the effects of sugars on the unfolding reaction. Despite the different approaches we arrive at the same conclusion: the increase in stability observed in the presence of sugars is primarily due to the increase in the free energy of creating the protein-solvent interface.

4.6. Calculation of preferential binding parameters

Timasheff developed a thermodynamic formalism that treats the effects of cosolutes on protein stability in terms of preferential interactions [5,6,8,9]. In the case of protein stabilizers, the cosolute is preferentially excluded from the protein's surface. The cosolute's concentration near the protein surface is lower than in the bulk. Any process such as unfolding, that increases the protein's solvent-exposed surface area is disfavored because exclusion of the cosolute from a larger surface area entails a correspondingly larger free energy cost. The amount of cosolute removed from the protein's vicinity is given by the preferential binding parameter, $(\partial m_3/\partial m_2)_{T,P,\mu_3}$ where m is the molality of species i, subscript 2 denotes the protein, and subscripts 1 and 3 denote water and cosolute, respectively. For cosolutes that are preferentially excluded this derivative is negative. The binding parameter is equal to the quantity measured experimentally by dialysis equilibrium within the approximation that $(\partial m_3/\partial m_2)_{T,P,\mu_3} = (\partial m_3/\partial m_2)_{T,\mu,\mu_3}$ [5]. The effect of a cosolute on the folding equilibrium is given by the difference in this parameter between the native and denatured states of the protein.

Due to the experimental difficulty associated with measuring the binding parameters for the denatured and native protein at the same conditions, Timasheff and coworkers have reported only values of the preferential binding parameter for the native state. The assumption is commonly made that the preferential binding parameter will scale with surface area as the protein unfolds. Implicitly this assumes that the chemical differences in the protein's surface between the native and denatured states are irrelevant. In fact, a cosolute being preferentially excluded from the native state doesn′t always result in the stabilization of that native state, as Timasheff has pointed out [60]. It is the difference in the preferential binding of a cosolute to the native and denatured states of a protein that determines its effect on stability. 2-Methyl-2,4-pentanediol and $MgCl_2$ have been shown to be preferentially excluded from the native state of proteins but these two cosolutes act as destabilizers because of their favorable interactions with the denatured state [60]. Therefore in order to determine a cosolute's impact on stability we need to either devise clever experiments to measure the preferential binding parameter for the denatured protein or we need to develop models that can predict the binding parameter for both states of the protein.

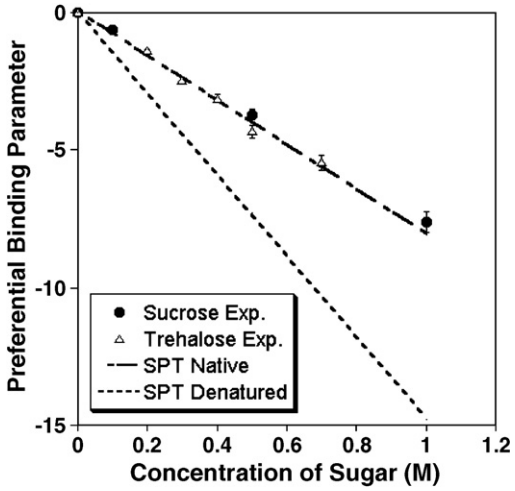

Fig. 4. The preferential binding parameter for RNase A with aqueous sugar solutions at 25 °C. Experimental data for the preferential binding of sucrose and trehalose (both disaccharides and thus similar in size) to native RNase A was taken from Refs. [8,9]. The dashed lines represent values of the binding parameter calculated using SPT for both the native and denatured states of RNase A using a sugar radius of 4.3 Å.

The preferential binding parameter can be calculated from SPT. To this end, one uses the thermodynamic identity [5]

$$\left(\frac{\partial m_3}{\partial m_2}\right)_{T,P,\mu_3} = -\frac{(\partial \mu_2/\partial m_3)_{T,P,m_2}}{(\partial \mu_3/\partial m_3)_{T,P,m_2}} \tag{14}$$

where μ_i and m_i are the chemical potential and molality of species i. SPT allows the calculation of the change in free energy of solvation of the protein with concentration of cosolute, i.e. the numerator of Eq. (14). The denominator of Eq. (14) represents the self-interaction of the cosolute. For sucrose, values of $(\partial \mu_3/\partial m_3)_{T,P,m_2}$ were taken from the work of Timasheff, who calculated this parameter from osmotic coefficient values of sucrose–water solutions [8]. Thus SPT along with knowledge of the cosolute's nonideality can be used to calculate the preferential binding parameter for both the native and denatured states of the protein. The binding parameter was calculated for RNase A in the presence of sucrose for both the native and denatured states. These results are shown in Fig. 4 along with experimentally determined values of the binding parameter for native RNase A in the presence of sucrose and trehalose. The calculated results are in excellent agreement with the experimentally determined values for the native state. There are no experimental data for denatured RNase at the same conditions to compare to the calculated values from SPT.

Both the experimental and theoretical values for the binding parameter are negative. This analysis shows that the sugar raises the chemical potential of the protein: $(\partial \mu_2/\partial m_3)_{T,P,\mu_1} > 0$. The presence of a cosolute molecule raises the protein's chemical potential, thus establishing a plausible driving force for its exclusion from the protein's surface. Fig. 4 shows that this effect is larger for the denatured protein: the preferential binding parameter is more negative and thus the number of sugar molecules excluded from the denatured state is greater. SPT explains this as being due to the fact that as the protein increases its surface area during unfolding, the free energy cost of inserting the protein into the sugar–water solution increases.

The preferential binding parameter can be related to the number of cosolute and water molecules found on average in the vicinity of the protein's surface, N_3 and N_1, respectively [61,62].

$$\left(\frac{\partial m_3}{\partial m_2}\right)_{T,P,\mu_3} = \langle N_3 \rangle_{1,N_1} - \frac{m_3}{m_1} N_1 \tag{15}$$

In the above equation, $\langle N_3 \rangle_{1,N_1}$ denotes the mean number of cosolute molecules in a control volume containing 1 protein molecule and N_1 solvent molecules. In other words the probability of having multiple protein molecules in a volume containing N_1 water molecules is negligible. When comparing the native and denatured state of the protein the minimum number of water molecules needed to define such a volume may be different. However we are free to choose N_1 for the native and denatured state of the protein to be equal as long as the chosen N_1 is greater than the minimum N_1 for both states and the probability of finding multiple protein molecules in the defined volume remains negligible. Then the difference in the preferential binding parameter for the native and denatured state of the protein is equal to the change in the number of sugar molecules excluded from the protein surface during unfolding, ΔN_3. From this analysis we calculate that in the presence of 1 M sucrose approximately 6–7 more sucrose molecules are excluded from the denatured state of RNase A compared to the native state.

5. Conclusions

Our findings show that SPT, despite its idealizations, is able to quantitatively describe the effects of sucrose and fructose on the thermal stability of RNase A and α-LA. The increase in stability in the presence of sugar, according to SPT, is due to an increase in the free energy of protein-solvent interface formation. We have also demonstrated that the magnitude of a sugar's impact on stability is highly dependent upon the denatured configuration of the protein. The conformation of denatured proteins can change significantly with solution conditions (pH, temperature, and ionic strength). The experimental techniques of CE, protein charge ladders, and dispersion analysis provide both thermodynamic and structural information that is essential for the microscopic interpretation of the effects of sugars on protein stability.

SPT can also be used to calculate preferential binding parameters in the case where enthalpic interactions between the protein and the cosolute are not important. The calculated binding parameters of sucrose to the native state of RNase A are in excellent agreement with experimental data. In addition we used SPT, and experimentally determined values of R_H to calculate values of the preferential binding parameter for sucrose to the denatured state of RNase A. This allows us to estimate the difference in number of sucrose molecules excluded from the denatured state compared to the native

state. Through the combination of experimental measurements of $\Delta G_{N\rightarrow D}$ and the change in protein configuration upon denaturation, and statistical mechanical analysis we have gained insight into the nature of the interactions between carbohydrate molecules and proteins in solution. This information can help guide the rational design of the formulation of protein pharmaceuticals and biocatalysts for improved shelf-life and stability.

The present work focuses on a class of cosolute molecules over a concentration range where the interactions between the protein and cosolute are predominantly entropic in nature. These entropic interactions are nonspecific in nature and do not depend upon the chemical nature of the cosolute molecule. Of course, enthalpic interactions cannot in general be ruled out. There are classes of cosolute molecules, most notably denaturants, where enthalpic interactions between the cosolute and the protein predominate. In the future we hope to combine our present experimental approach with a statistical mechanical analysis that combines entropic and enthalpic interactions to gain insight into the interactions between proteins and a broader range of cosolute molecules.

Acknowledgements

P.G.D. gratefully acknowledges the support of the Department of Energy, Division of Chemical Sciences, Geosciences and Biosciences, Office of Basic Energy Sciences, Grant No. DE-FG02-87ER13714, and of the National Science Foundation through Collaborative Research in Chemistry Grant No. CHE 0404699.

References

[1] J.H. Crowe, L.M. Crowe, Preservation of mammalian cells-learning nature's tricks, Nat. Biotechnol. 18 (2000) 145–146.
[2] S.B. Zimmerman, S.O. Trach, Estimation of macromolecule concentrations and excluded volume effects for the cytoplasm of *Escherichia coli*, J. Mol. Biol. 222 (1991) 599–620.
[3] R.J. Ellis, A.P. Minton, Cell biology: join the crowd, Nature 425 (2003) 27–28.
[4] P.R. Davis-Searles, A.J. Saunders, D.A. Erie, D.J. Winzor, G.J. Pielak, Interpreting the effects of small uncharged solutes on protein-folding equilibria, Annu. Rev. Biophys. Biomol. Struct. 30 (2001) 271–306.
[5] S.N. Timasheff, The control of protein stability and association by weak interactions with water: how do solvents affect these processes, Annu. Rev. Biophys. Biomol. Struct. 22 (1993) 67–97.
[6] S.N. Timasheff, Control of protein stability and reactions by weakly interacting cosolvents: the simplicity of the complicated, Adv. Protein Chem. 51 (1998) 355–432.
[7] G. Scatchard, Physical chemistry of protein solutions. I. Derivation of the equations for the osmotic pressure, J. Am. Chem. Soc. 68 (1946) 2315–2319.
[8] J.C. Lee, S.N. Timasheff, The stabilization of proteins by sucrose, J. Biol. Chem. 256 (1981) 7193–7201.
[9] G. Xie, S.N. Timasheff, The thermodynamic mechanism of protein stabilization by trehalose, Biophys. Chem. 64 (1997) 25–43.
[10] K. Gekko, S.N. Timasheff, Mechanism of protein stabilization by glycerol: preferential hydration in glycerol–water mixtures, Biochemistry 20 (1981) 4667–4676.
[11] A.P. Minton, The effect of volume occupancy upon the thermodynamic activity of proteins — some biochemical consequences, Mol. Cell. Biochem. 55 (1983) 119–140.
[12] D. Hall, A.P. Minton, Macromolecular crowding: qualitative and semiquantitative successes, quantitative challenges, Biochim. Biophys. Acta 1649 (2003) 27–139.
[13] A.J. Saunders, P.R. Davis-Searles, D.L. Allen, G.J. Pielak, D.A. Erie, Osmolyte-induced changes in protein conformational equilibria, Biopolymers 53 (2000) 293–307.
[14] J.A. Schellman, Protein stability in mixed solvents: a balance of contact interaction and excluded volume, Biophys. J. 85 (2003) 108–125.
[15] T.P. Creamer, R. Srinivasan, G.D. Rose, Modeling unfolded states of proteins and peptides. II. Backbone solvent accessibility, Biochemistry 36 (1997) 2832–2835.
[16] H. Reiss, H.L. Frisch, E. Helfland, J.L. Lebowitz, Aspects of the statistical thermodynamics of real fluids, J. Chem. Phys. 32 (1960) 119–124.
[17] K.E. Shearwin, D.J. Winzor, Thermodynamic nonideality as a probe of reversible protein unfolding effected by variations in pH and temperature: studies of ribonuclease, Arch. Biochem. Biophys. 282 (1990) 297–301.
[18] T.F. O'Connor, P.G. Debenedetti, J.D. Carbeck, Simultaneous determination of structural and thermodynamic effects of carbohydrate solutes on the thermal stability of ribonuclease A, J. Am. Chem. Soc. 126 (2004) 11794–11795.
[19] J.D. Carbeck, I.J. Colton, J.M. Gao, G.M. Whitesides, Protein charge ladders, capillary electrophoresis, and the role of electrostatics in biomolecular recognition, Acc. Chem. Res. 31 (1998) 343–350.
[20] R.S. Negin, J.D. Carbeck, Measurement of electrostatic interactions in protein folding with the use of protein charge ladders, J. Am. Chem. Soc. 124 (2002) 2911–2916.
[21] U. Sharma, R.S. Negin, J.D. Carbeck, Effects of cooperativity in proton binding on the net charge of proteins in charge ladders, J. Phys. Chem., B 107 (2003) 4653–4666.
[22] D.C. Henry, The cataphoresis of suspended particles. Part I. The equation of cataphoresis, Proc. R. Soc. Lond. 133 (1931) 106–129.
[23] D.J. Winzor, S. Jones, S.E. Harding, Determination of protein charge by capillary zone electrophoresis, Anal. Biochem. 333 (2004) 225–229.
[24] F. Kalman, S. Ma, R.O. Fox, C. Horvath, Capillary electrophoresis of S-nuclease mutants, J. Chromatogr., A 705 (1995) 135–154.
[25] I.J. Colton, J.R. Anderson, J.M. Gao, R.G. Chapman, L. Isaacs, G.M. Whitesides, Formation of protein charge ladders by acylation of amino groups on proteins, J. Am. Chem. Soc. 119 (1997) 12701–12709.
[26] U. Sharma, N.J. Gleason, J.D. Carbeck, Diffusivity of solutes measured in glass capillaries using Taylor's analysis of dispersion and a commercial CE instrument, Anal. Chem. 77 (2005) 806–813.
[27] G.I. Taylor, Dispersion of soluble matter in solvent flowing slowly through a tube, Proc. R. Soc. Lond., Ser. A 219 (1953) 186–203.
[28] G.I. Taylor, Conditions under which dispersion of a solute in a stream of solvent can be used to measure molecular diffusion, Proc. R. Soc. Lond., Ser. A 225 (1954) 473–477.
[29] V.J. Hilser, G.D. Worosila, E. Freire, Analysis of thermally induced protein folding unfolding transitions using free solution capillary electrophoresis, Anal. Biochem. 208 (1993) 125–131.
[30] Y. Ishihama, Y. Oda, N. Asakawa, M. Iwakura, Nano-scale monitoring of the thermally induced unfolding of proteins using capillary electrophoresis with in-column incubation, Anal. Sci. 13 (1997) 931–938.
[31] K.A. McIntosh, W.N. Charman, S.A. Charman, The application of capillary electrophoresis for monitoring effects of excipients on protein conformation, J. Pharm. Biomed. Anal. 16 (1998) 1097–1105.
[32] D. Rochu, G. Ducret, F. Ribes, S. Vanin, P. Masson, Capillary zone electrophoresis with optimized temperature control for studying thermal denaturation of proteins at various pH, Electrophoresis 20 (1999) 1586–1594.
[33] E. Stellwagen, C. Gelfi, P.G. Righetto, Protein folding observed by capillary electrophoresis in isoelectric buffers, J. Chromatogr., A 838 (1999) 131–138.
[34] B. Verzola, F. Chiti, G. Manao, P.G. Righetti, Monitoring equilibria and kinetics of protein folding/unfolding reactions by capillary zone electrophoresis, Anal. Biochem. 282 (2000) 239–244.
[35] B. Verzola, F. Fogolari, P.G. Righetti, Monitoring folding/unfolding transitions of proteins by capillary zone electrophoresis: measurements of

ΔG and its variations along the pH scale, Electrophoresis 22 (2001) 3728–3735.
[36] E.D. Lorenzi, S. Grossi, G. Massolini, S. Giorgetti, P. Mangione, A. Andreola, F. Chiti, V. Bellotti, G. Caccialanza, Capillary electrophoresis investigations of a partially unfolded conformation of β-microglobulin, Electrophoresis 23 (2002) 918–925.
[37] P.G. Righetti, B. Verzola, Folding/unfolding/refolding of proteins: present methodologies in comparison with capillary zone electrophoresis, Electrophoresis 22 (2001) 2359–2374.
[38] L.C. Wu, P.S. Kim, A specific hydrophobic core in the α-lactalbumin molten globule, J. Mol. Biol. 280 (1998) 175–182.
[39] C. Redfield, B.A. Schulman, M.A. Milhollen, P.K. Kim, C.M. Dobson, α-lactalbumin forms compact molten globule in the absence of disulfide bonds, Nat. Struct. Biol. 6 (1999) 948–952.
[40] E.A. Permyakov, L.A. Morozova, E.A. Burstein, Cation binding effects on the pH, thermal and urea denaturation transitions in α-lactalbumin, Biophys. Chem. 21 (1985) 21–31.
[41] D.L. Allen, G.J. Pielak, Baseline length and automated fitting of denaturation data, Protein Sci. 7 (1998) 1262–1263.
[42] C.N. Pace, G.R. Grimsley, S.T. Thomas, G.I. Makhatadze, Heat capacity change for ribonuclease A folding, Protein Sci. 8 (1999) 1500–1504.
[43] Y.V. Griko, E. Freire, P.L. Privalov, Energetics of the α-lactalbumin states-A calorimetric and statistical thermodynamic study, Biochemistry 33 (1994) 1889–1899.
[44] K. Sasahara, P. McPhie, A.P. Minton, Effect of dextran on protein stability and conformation attributed to macromolecular crowding, J. Mol. Biol. 326 (2003) 1227–1237.
[45] M.K. Menon, A.L. Zydney, Determination of effective protein charge by capillary electrophoresis: effects of charge regulation in the analysis of charge ladders, Anal. Chem. 72 (2000) 5714–5717.
[46] J.A. Caravella, J.D. Carbeck, D.C. Duffy, G.M. Whitesides, B. Tidor, Long-range electrostatic contributions to protein-ligand binding estimated using protein charge ladders, affinity capillary electrophoresis, and continuum electrostatic theory, J. Am. Chem. Soc. 121 (1999) 4340–4347.
[47] J. Gao, M. Mammem, G.M. Whitesides, Evaluating electrostatic contributions to binding with the use of protein charge ladders, Science 272 (1996) 535–537.
[48] Y. Qu, C.L. Bolen, D.W. Bolen, Osmolyte-driven contraction of a random coil protein, Proc. Natl. Acad. Sci. U. S. A. 95 (1998) 9268–9273.
[49] O.G. Berg, The influence of macromolecular crowding on thermodynamic activity: solubility and dimerization constants for spherical and dumbbell-shaped molecules in a hard-sphere mixture, Biopolymers 30 (1990) 1027–1037.
[50] K.E.S. Tang, V.A. Bloomfield, Excluded volume in solvation: sensitivity of scaled-particle theory to solvent size and density, Biophys. J. 79 (2000) 2222–2234.
[51] J.K. Kaushik, R.J. Bhat, Thermal stability of proteins in aqueous polyol solutions: role of the surface tension of water in the stabilizing effects of polyols, J. Phys. Chem. 102 (1998) 7058–7066.
[52] D.J. Winzor, C.L. Ford, L.W. Nichol, Thermodynamic nonideality as a probe of macromolecular isomerizations — application to the acid expansion of bovine serum–albumin, Arch. Biochem. Biophys. 234 (1984) 15–23.
[53] P.R. Davis-Searles, A.S. Morar, A.J. Saunders, D.A. Erie, G.J. Pielak, Sugar-induced molten-globule model, Biochemistry 37 (1998) 17048–17053.
[54] A.P. Minton, Models for excluded volume interactions between an unfolded protein and rigid macromolecular cosolute: macromolecular crowding and protein stability revisited, Biophys. J. 88 (2005) 971–985.
[55] K.A. Dill, D. Shortle, Denatured states of proteins, Ann. Rev. Biochem. 60 (1991) 795–825.
[56] R.J. Corbett, R.S. Roche, Use of high-speed size-exclusion chromatography for the study of protein folding and stability, Biochemistry 23 (1984) 1888–1894.
[57] H. Reiss, Scaled particle methods in the statistical thermodynamics of fluids, Adv. Chem. Phys. 9 (1966) 1–84.
[58] T.Y. Lin, S.N. Timasheff, On the role of surface tension in the stabilization of globular proteins, Protein Sci. 5 (1996) 372–381.
[59] B.M. Baynes, B.L. Trout, Proteins in mixed solvents: a molecular-level perspective, J. Phys. Chem., B 107 (2003) 14058–14067.
[60] T. Arakawa, R. Bhat, S.N. Timasheff, Why preferential hydration does not always stabilize the native structure of globular proteins, Biochemistry 29 (1990) 1924–1931.
[61] H. Inoue, S.N. Timasheff, Preferential and absolute interactions of solvent components with proteins in mixed solvent systems, Biopolymers 11 (1972) 737–743.
[62] S.N. Timasheff, H. Inoue, Preferential binding of solvent components to protein in mixed water-organic solvent systems, Biochemistry 7 (1968) 2501–2513.